Available online at www.sciencedirect.com

SciVerse ScienceDirect

Current Opinion in Structural Biology

Red fluorescent proteins: chromophore formation and cellular applications

Atsushi Miyawaki[1,2], Daria M Shcherbakova[3,4] and Vladislav V Verkhusha[3,4]

In the last decade, a number of red fluorescent proteins (RFPs) that emit orange, red, and far-red fluorescence have been isolated from anthozoans (corals), and developed through directed molecular evolution. An attractive property possessed by some RFPs is that their red fluorescence can be turned on or modulated by illumination at specific wavelengths. Recent progress in the development of RFPs has been accompanied with detailed studies of chromophore chemistry. A thorough understanding of the molecular mechanisms involved in the post-translational modifications of red chromophores would enable scientists to design RFPs with the desired properties to advance imaging applications. This article provides a broad perspective on the chemistry and applications of RFPs.

Addresses
[1] Brain Science Institute, RIKEN, 2-1 Hirosawa, Wako-city, Saitama 351-0198, Japan
[2] Life Function and Dynamics, ERATO, JST, 2-1 Hirosawa, Wako-city, Saitama 351-0198, Japan
[3] Department of Anatomy and Structural Biology, Albert Einstein College of Medicine, 1300 Morris Park Avenue, Bronx, NY 10461, United States
[4] Gruss-Lipper Biophotonics Center, Albert Einstein College of Medicine, 1300 Morris Park Avenue, Bronx, NY 10461, United States

Corresponding authors: Miyawaki, Atsushi (matsushi@brain.riken.jp), Verkhusha, Vladislav V (vladislav.verkhusha@einstein.yu.edu)

Current Opinion in Structural Biology 2012, **22**:679–688

This review comes from a themed issue on **Biophysical methods**

Edited by **S Samar Hasnain** and **Soichi Wakatsuki**

For a complete overview see the Issue and the Editorial

Available online 20th September 2012

0959-440X/$ – see front matter,

http://dx.doi.org/10.1016/j.sbi.2012.09.002

Introduction

Technological innovations that have emerged from the molecular cloning of GFP (green fluorescent protein) from the jellyfish *Aequorea victoria* (*Aequorea* GFP) in 1992 have played a significant role in advancing our ability to unravel the fine details of a wide range of biological functions [1]. The earliest spectral variants of *Aequorea* GFP exhibited blue, cyan, and yellowish-green emissions, but until 2008 [2], none possessed emission maxima longer than 529 nm. The discovery of novel GFP-like proteins from other animals in 1999 [3•] has significantly expanded the range of colors to include red; these newer red molecules are now available for biological applications [4–7]. Despite their modest sequence similarity with *Aequorea* GFP, these GFP-like proteins share common structural organization [8••]. An intrinsic chromophore forming from a central helix is shielded within a β-can fold (an 11-stranded β-barrel).

In this review, we will describe both the physicochemical and practical characteristics of the GFP-like proteins that emit yellow, orange, red, and far-red fluorescence in their final matured states (RFPs). Most of these molecules are derived from anthozoans. We focus on RFPs because an early model, in which the maturation of the DsRed-like red chromophore proceeds via a green GFP-like chromophore intermediate [9], has recently been revised [10–12]. Furthermore, a growing number of biologists await the development of superior RFPs for use in deep-tissue and whole-body imaging. We will aim at concise explanations; detailed mechanisms and applications have been reviewed recently elsewhere [6,7,8••].

RFPs fall into two families, as shown in Figure 1: DsRed (pink background) and Kaede (green background). The figure illustrates how the chromophore structures of these RFPs arose by evolution (solid arrows) or engineering (dotted arrows). All RFPs introduced here share X–Tyr–Gly, a chromophore-forming tripeptide; thus, all the chromophores shown in Figure 1 possess a phenol ring derived from the Tyr residue. DsRed and DsRed-like RFPs are the prototype DsRed family members. These prototypes can produce yellow-emitting, orange-emitting, and far-red-emitting RFPs; RFPs with large Stokes shifts; and photomodulatable RFPs. It should be noted that these chromophores' spectral properties are often determined by the equilibrium between the protonated and deprotonated states of the phenol hydroxyl group. However, because chromophore development is catalyzed by the whole protein, further spectral diversity can arise from the protein cavity that holds the chromophore.

DsRed-like RFPs

The red chromophore of DsRed derived from *Discosoma* and related species represents an extended GFP-like core, with an additional desaturated C_α–N bond at a position 65 that forms an N-acylimine (C=N–C=O). Extended π-electron conjugation results in red-shifted absorbance and emission. Initially, the red chromophore of DsRed was thought to arise from a green GFP-like

Figure 1

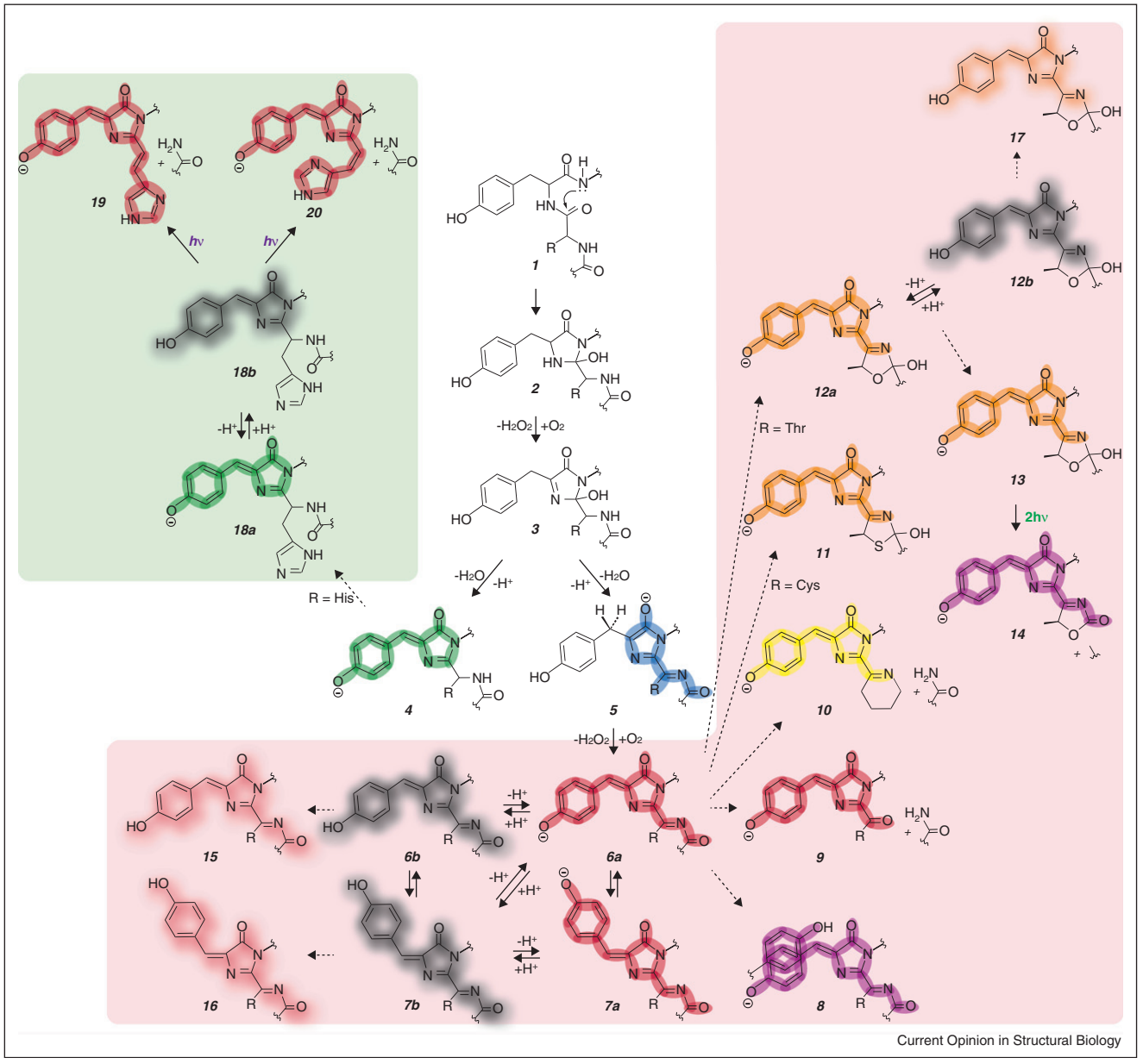

Chemical transformations of the chromophores in RFPs. The DsRed and Kaede families are shown with pink and green backgrounds, respectively. π-conjugation for visible-light absorption that results in a substantial amount of fluorescence is indicated by colored shading; gray shading denotes nonfluorescence. Solid arrows indicate autocatalytic or photo-induced modifications. Anti-parallel solid arrows indicate *cis–trans* isomerizations or equilibriums between ionized (*a*) and protonated (*b*) states. Dotted arrows indicate chromophore transformations resulted from mutagenesis of the amino acid residues surrounding the chromophore. Consequently, for example, chromophores *6b* and *15* may have different degrees of electron conjugation despite the same chemical structures. This applies to chromophores *7b* and *16*, chromophores *12a* and *13*, and chromophores *12b* and *17*. The green-emitting chromophore of *Aequorea* GFP, 4-(*p*-hydroxybenzylidene)-5-imidazolinone, is shown as chromophore *4*. The internal tripeptide, Ser65–Tyr66–Gly67, forms the chromophore by nucleophilic attack of Gly67-N_α on the carbonyl group of Ser65, followed by dehydration and oxidation of the C_α–C_β bond of Tyr66 (*1* → *2* → *3* → *4*). From a more detailed perspective, however, *Aequorea* GFP maturation is best described by a cyclization–oxidation–dehydration sequence. By contrast, maturation of red-emitting chromophores involves a formation of N-acylimine by desaturation of C_α65–N65 bond at the first stage before the formation of double bond between C_α and C_β of Tyr66 (*1* → *2* → *3* → *5* → *6a*). The chemical structures with colored clouds (*15*, *16*, and *17*) denote the protonated chromophores that transform to emitting anionic forms via the ESPT pathway. *hν*, photon.

chromophore (*4* → *6a*) [9]. In the most current model, however, the green GFP-like chromophore is the end product; it is suggested that the maturation of the red chromophore proceeds via a blue-emitting intermediate similar to mTagBFP [12] and mTagBFP2 [13] chromophores (*5* → *6a*). Crystallographic and mass spectrometric analysis of several FPs including PAmCherry [14], mCherry-based fluorescent timers (FTs) [10], and mTagBFP [12], along with electronic structure calculations [15•], has shown that the blue intermediate possesses a chromophore composed of the anionic derivative of N-[(5-hydroxy-1H-imidazole-2yl)methylidene]acetamide (*5*) [15•]. Then, additional conjugation of the mTagBFP-like blue chromophore with the phenolic ring of Tyr66 results in the maturation of the red chromophore.

It is suggested [15•] that the product formed after the cyclization and oxidation (structure *3*) serves as the branch point between the green and red pathways [7,12]. In another model, the cyclic imine form is proposed to represent the branch point intermediate [11]. In either case, however, the formation of the N-acylimine double bond competes with the formation of the double bond between C_α and C_β of Tyr66 in chromophore *3* or a similar structure. Therefore, in order to generate an ideal DsRed-like RFP, N-acylimine formation should be overwhelmingly favored; otherwise, the fluorescence signal produced by DsRed-like RFP would contain a green component, prohibiting the use of this protein in combination with green-emitting fluorophores in dual-color labeling experiments. Furthermore, providing that generation of the green byproduct is negligible, fast conversion from the blue chromophore to the red one will lead to both efficient labeling by red fluorescence and less contamination by blue fluorescence. Such precocious DsRed-like RFPs include mCherry [16]. Conversely, slow but complete blue-to-red conversion can also be advantageous, especially for the analysis of the duration of gene expression in cells. Several slowly maturing DsRed-like RFPs that change color from blue to red with predictable time courses can serve as fluorescent timers (FTs) [17]. This feature allows for ratiometric analysis of the blue-to-red emission, providing an estimate of the time elapsed after initiation of reporter gene expression. Key amino acids in the chromophore environment critical for the timing properties of FTs have been identified, enabling development of Fast-FT, Medium-FT, and Slow-FT versions.

Yellow-emitting, orange-emitting, and far-red-emitting RFPs

The DsRed-like chromophore (*6*) can undergo various chemical transitions that change the fluorescence color. Cyclization of the N-acylimine group results in generation of a third ring in addition to 4-(*p*-hydroxybenzylidene)-5-imidazolinone. RFPs possessing these chromophore modifications include zFP538 (*10*) [18], mKO (*11*) [19], and mOrange (*12*) [20]. In zFP538, the N-acylimine is attacked by the terminal amino group of Lys65 to form a new six-membered ring, cleaving the polypeptide backbone with ejection of a carboxamide. In mKO or mOrange, the nucleophilic addition of a Thr65 hydroxyl or a Cys65 thiolate onto the N-acylimine carbonyl carbon produces a new five-membered ring: an oxazole ring or a thiazoline ring, respectively. In all these cases, the conjugated π-electron systems are less extended than in DsRed; consequently, zFP538 emits yellow fluorescence, whereas mKO and mOrange emit orange fluorescence. By contrast, hydrolysis of the N-acylimine group of the DsRed-like chromophore (*6*) results in a main chain break immediately preceding the chromophore tripeptide, and a formation of the asFP595-like chromophore (*9*) [21], without a substantial change in color.

The excitation and emission wavelengths of the DsRed-like chromophore (*6*) are further modified by its surrounding amino acids (*8*). The far-red-emitting chromophores of mRouge [22], E2-Crimson [23], mNeptune [24], and TagRFP657 [25] are generated by the formation of hydrogen bonding, stacking interactions, and/or hydrophobic residues surrounding the DsRed-like chromophore. Among cell biologists, there has been increasing demand for superior RFPs with excitation and emission maxima in the far-red range. Since longer-wavelength light scatters less, and thus can travel further than shorter-wavelength light, far-red-emitting RFPs are desirable for applications involving deep fluorescence imaging.

RFPs with a large Stokes shift

Several RFPs possessing a large Stokes shift (LSS) have been developed. An LSS can result from an excited-state proton transfer (ESPT) that transforms the excited neutral form of the chromophore to the emitting anionic form [26•]. The LSS RFP named Keima, which absorbs and emits light maximally at 440 nm and 620 nm, respectively, was constructed from a coral fluorescent protein (*15*) [27]. Combining a monomeric version of Keima with cyan-emitting fluorescent protein allows dual-color fluorescence cross-correlation spectroscopy (FCCS) using a single 458-nm laser line, as well as complete separation of the fluorescent protein emissions. Furthermore, a large set of spectrally different fluorescent proteins, including Keima and its orange-emitting variant Keima570, can be excited with a single laser line for use in simultaneous multicolor imaging [27].

It should be noted that Keima has a bimodal excitation spectrum with peaks at 440 nm and 586 nm, respectively corresponding to the neutral and ionized states of the chromophore's phenolic hydroxyl moiety. pH titration experiments confirmed that the neutral and ionized states predominate at high and low pH values, respectively, with a pK_a value of 6.5 [27]. The presence of the 586-nm excitation peak of Keima may prevent multicolor

applications in combination with RFPs that are excited near 586 nm. To overcome this challenge, two LSS fluorescent proteins with exclusively neutral chromophores in the ground states have been developed from a parental RFP, mKate; these derivatives were named LSSmKate1 (*15*) and LSSmKate2 (*16*) [28]. In each protein, the stabilization of the chromophore in neutral form in the ground state was successfully achieved by placement of carboxyl groups in the vicinity of the chromophore. Both proteins have single-peaked spectra, with excitation at 463 nm and emission at 624 nm (LSSmKate1) or excitation at 460 nm and emission at 605 nm (LSSmKate2). Importantly, it is possible to engineer the ESPT pathway in other RFPs by introducing carboxyl groups near the chromophore. Such rational mutagenesis was performed on mOrange to create LSSmOrange (excitation/emission at 437/572 nm) (*17*) [29]. LSSmOrange has been used as a FRET donor, in combination with mKate2 (excitation/emission at 588/633 nm) as an acceptor. Furthermore, dual FRET imaging with single-wavelength excitation was achieved using the LSSmOrange/mKate2 FRET pair in combination with the conventional CFP/YFP FRET pair (Figure 2) [29].

In contrast to the stable neutral chromophores in the ground states of LSSmKate1, LSSmKate2, and LSSmOrange, the pH-dependent bimodal excitation spectrum of Keima can be used to detect the pH gradient across lysosomal membranes. Upon the fusion of autophagosomes with lysosomes in autophagic events, cytosolic components and organelles encapsulated by autophagosomes are exposed to acidic pH and lysosomal proteases [30]. Importantly, most fluorescent proteins derived from corals retain fluorescence in these harsh environments; by contrast, *Aequorea* GFP and its variants are efficiently degraded by lysosomal proteases [31•]. Thus, because it can survive in lysosomes and emit differently colored signals at acidic and neutral pH values, Keima can provide a cumulative readout of autophagic activity [32].

Photomodulatable RFPs

Photoactivatable RFPs are initially non-fluorescent, but exhibit bright red fluorescence after UV or violet light illumination [33,34]. Examples include PAmCherry (*7a*) [35], PATagRFP (*7a*) [36•], and PAmKate (*6a*) [37]. Crystallographic and mass spectroscopic analyses have revealed that in the dark state, the chromophore of PAmCherry adopts a non-planar configuration similar to the structure of the mTagBFP chromophore, with a single non-oxidized C_α–C_β bond at Tyr66 (similar to *5*); photon absorption results in the oxidation of the Tyr66 C_α–C_β bond followed by decarboxylation of Glu222 residue [14].

To overcome the diffraction barrier of light, many methods have been developed to temporally separate molecules that would otherwise be spatially indistinguishable; these approaches are collectively known as super-resolution imaging. These methods include fluorescence photoactivated localization microscopy (PALM [38] or FPALM [39]), which uses photoactivatable or photoconvertible fluorescent proteins. PALM can be combined with single-particle tracking in live cells. This technique, called single-particle tracking PALM (sptPALM), allows the localization and tracking of many overlapping trajectories, because the distance between fluorescent molecules in any single frame is several times greater than the width of the point-spread function. The resulting high density of dynamic information provides a spatially resolved map of single-molecule diffusion constants. In an example of dual-color sptPALM, Subach *et al.* monitored the dynamics of two different single transmembrane proteins fused to PATagRFP and PAGFP in the same cell [36•].

A fraction of mOrange becomes far-red emitting after irradiation with 458 nm or 488 nm; this feature has been augmented by mutagenesis to yield PSmOrange (*13*) [40] and PSmOrange2 [41], which changes color from orange to far-red with high contrast following irradiation with blue-green light. The photoswitching occurs via a two-step photo-oxidation process that causes cleavage of the polypeptide backbone. The far-red fluorescence of photoconverted PSmOrange results from a new type of chromophore containing an N-acylimine with a co-planar carbon-oxygen double bond (*14*). By contrast, the N-acylimine group in the DsRed-like chromophore (*6a*) and its derivatives (*6b*, *7a*, *7b*, *8*, *15*, *16*) is not co-planar. Two photoswitching proteins that can be used in combination are cyan-to-green photoswitchable CFP2 (PSCFP2) and PSmOrange (or PSmOrange2), which are photoconverted by violet light and blue-green light, respectively. They can be utilized to differentially highlight two distinct proteins and simultaneously image the converted and unconverted populations of each (Figure 3) [40].

Reversible photoswitching between the non-fluorescent and fluorescent state has been observed for some RFPs [42,43], such as rsTagRFP (*6a* ↔ *7b*), rsCherry (*6a* ↔ *7a*), and rsCherryRev (*6a* ↔ *7a*). It was found that light-induced *cis–trans* isomerization of the chromophore accompanied by its protonation/deprotonation is involved in the photoswitching mechanism of rsTagRFP [44].

Kaede family

Kaede, a natural fluorescent protein found in the stony coral *Trachyphyllia geoffroyi*, irreversibly changes its emission wavelength from green (518 nm) (*18a*) to red (582 nm) (*19*) upon irradiation at ~400 nm [45]. This large shift in emission wavelength enables high contrast in fluorescence highlighting. Other examples of naturally occurring photoconvertible fluorescent proteins include EosFP [46], dendFP [47], mcavRFP [48], and rfloRFP [48], found respectively in the corals *Lobophyllia hemprichii*, *Dendronephthya*, *Monastrea cavernosa*, and *Ricordea florida*. Studies of these proteins have posed intriguing

Figure 2

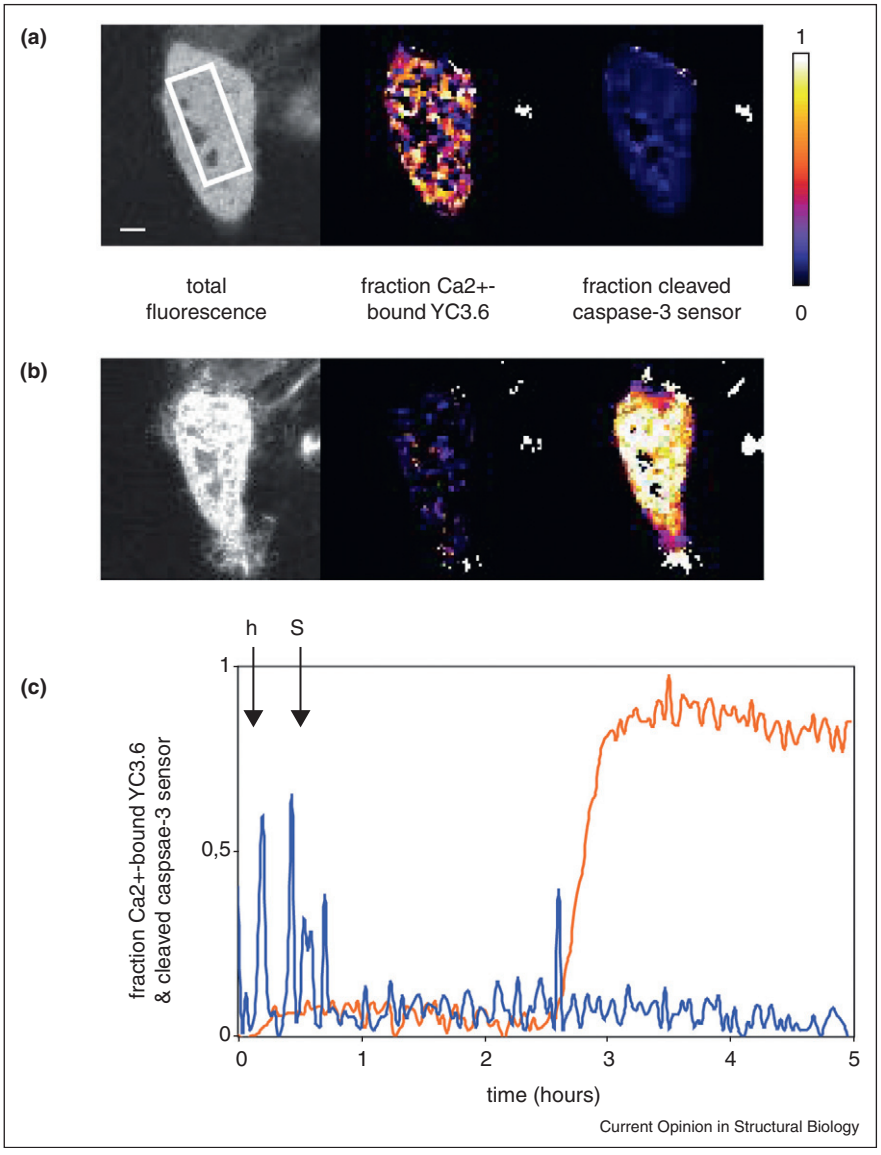

Single excitation wavelength dual FRET sensor imaging in transfected HeLa cells. **(a, b)** HeLa cell coproducing the calcium sensor YC3.6 [59] and the LSSmOrange-mKate2 caspase-3 biosensor, 10 min after addition of histamine (h) to the medium **(a)** and 4 hours after starting the experiment **(b)**. The cells were stimulated with staurosporine (s) after 30 min. The left panels show the total fluorescence intensity. The middle panels represent the fraction of Ca^{2+}-bound YC3.6 sensor to the total amount of YC3.6 sensor, and the right panels display the fraction of active, cleaved capase-3 sensor to the total amount of caspase-3 sensor. To reduce background contributions, the fraction images have been multiplied with a binary mask of the intensity image. Scale bar, 3 μm. **(c)** Temporal evolution of the sensor-activities in a region within the cell, indicated by the white box. The curves represent the fraction of Ca^{2+}-bound YC3.6 sensor (blue) and the fraction of cleaved capase-3 biosensor (orange).
Courtesy of M.A. Hink and Th.W.J. Gadella, University of Amsterdam, Netherlands.

questions about the significance of color variations occurring within individual coral animals. When exposed to sunlight, the tentacles and disks of coral animals turn red in proportion to the degree of photoconversion; they subsequently revert to their original colors as newly synthesized proteins are added. Mechanisms such as this may be responsible for the great variety of color observed in coral reefs.

In all of these Kaede family members, a unique tripeptide, His62–Tyr63–Gly64, forms a green chromophore that can be photoconverted to a red one. Mutagenesis studies have revealed that the first His62 is required, but not sufficient, for photoconversion [49•]. The conversion of an ordinary fluorescent protein into a photoconvertible one represents a significant protein engineering challenge, which was met by the creation of KikGR [50].

Figure 3

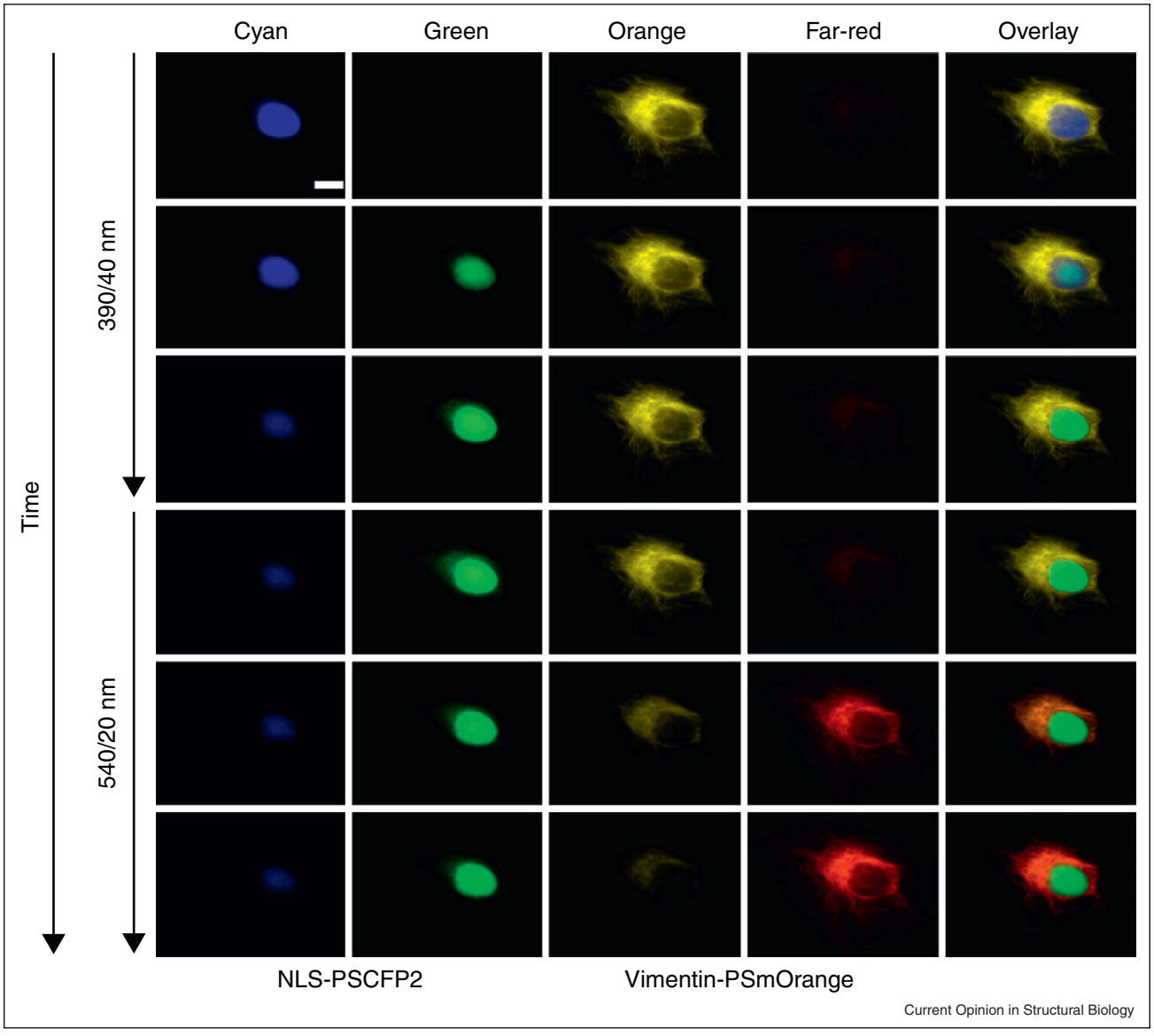

Differential photoswitching of PSCFP2 and PSmOrange co-expressed in a live mammalian cell [40]. The nucleus-localized NLS-PSCFP2 was photoswitched from a cyan form to a green form with 390/40 nm light. The vimentin-PSmOrange fusion protein was photoswitched from an orange form to a far-red form with 540/20 nm light. Photoswitching time for each was 14 s. Scale bar, 10 μm.

Tsutsui *et al.* cloned a new green-emitting GFP-like protein (KikG), which contains Asp62–Tyr63–Gly64, from the coral *Favia favus*, and determined its crystal structure. They replaced Asp62–Tyr63–Gly64 with His62–Tyr63–Gly64, and introduced numerous additional mutations chosen on the basis of the crystal structure, ultimately obtaining a photoconvertible version of KikG (KikGR).

The photoconversion process occurs via a β-elimination reaction that causes cleavage of the His62 N_α–C_α bond and subsequent extension of the π-conjugated system [49•,51]. It should be noted that the cleavage of the His62 N_α–C_α bond releases a carboxamide-containing peptide as a leaving group, which is rarely seen in a conventional β-elimination reaction (Figure 4). The molecular mechanism that makes this reaction possible has remained unclear. Although X-ray crystallography, NMR, and mass spectroscopy have been employed to compare chromophore structures before and after the reaction, these analyses did not directly probe the nature and structure of the reaction's intermediate states.

Figure 4

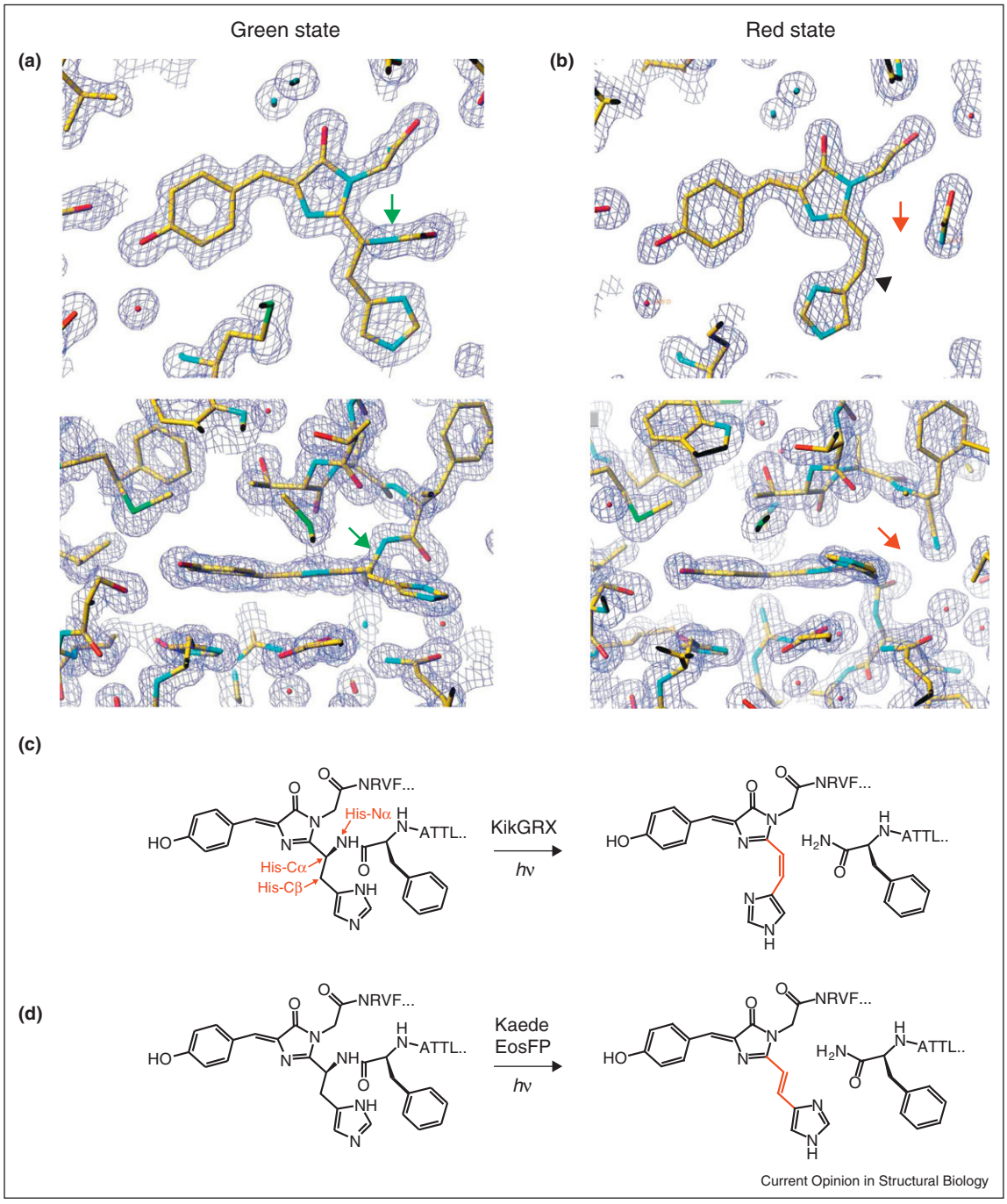

Structural basis for the green-to-red conversion. **(a)** Electron density maps (2Fo-Fc at 1.5σ) showing the chromophore structure of the green-emitting (unconverted) state viewed from the top (top panel) and side (bottom panel) of the chromophore plane. **(b)** The structure of the red (converted) state viewed from the top (top panel) and side (bottom panel) of the chromophore plane. Electron density connecting His62-C_α and His62-N_α exists in **(a)** (green arrows), but not in **(b)** (red arrows). The red arrowhead indicates the *cis* configuration of the C=C double bond in the (5-imidazolyl)ethenyl group of the red-emitting chromophore. **(c, d)** Summary of β-elimination and extension of the π-conjugated system in KikGRX **(c)** or Kaede and EosFP **(d)**. The structures derived from Phe61, His62, Tyr63, and Gly64 are drawn; the neighboring amino acids (single-letter code) are also shown. C=C double bonds in the (5-imidazolyl)ethenyl group and the neighboring bonds are colored in red in chromophores of the red states.

Figure 5

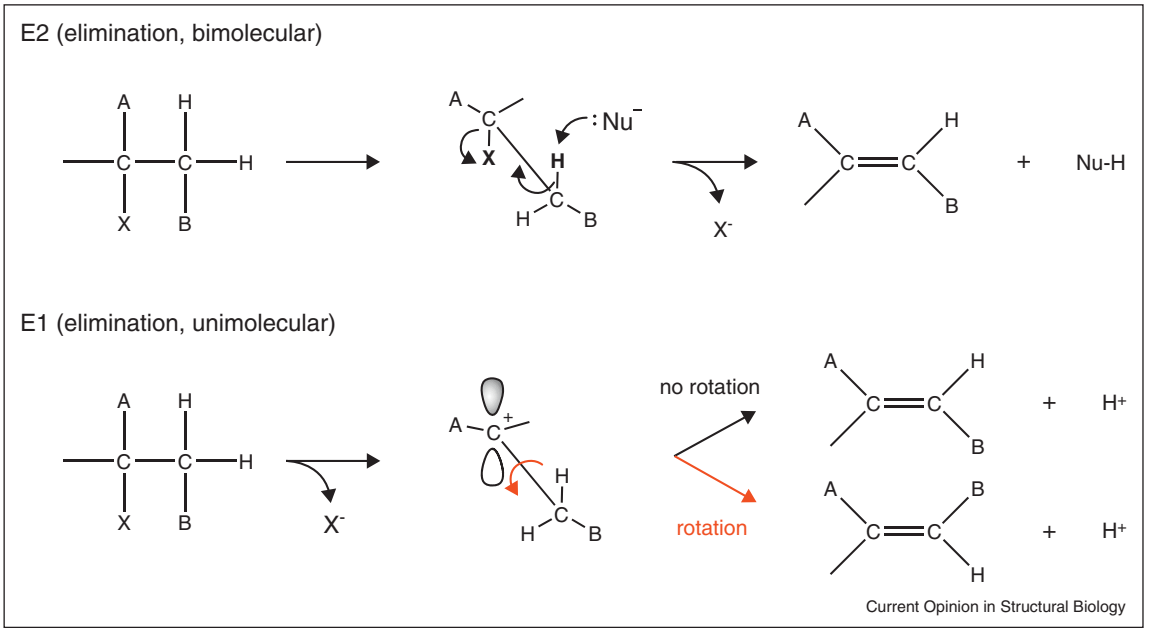

Scheme for E2 and E1 elimination reactions.

In general, there are two basic mechanisms for a β-elimination reaction: E2 (*elimination*, *bimolecular*) and E1 (*elimination*, *unimolecular*) (Figure 5). In the E2 elimination reaction, abstraction of a proton by a base and loss of the neighboring leaving group occur simultaneously, yielding a single product with a single isomeric configuration. Since the abstraction of a proton is a major driving force for the E2 mechanism, a strong base is generally required to initiate the reaction. In the E1 mechanism, by contrast, loss of the leaving group occurs first, resulting in formation of a carbocation intermediate. At that stage on the reaction pathway, structural rearrangement can occur on the carbocation intermediate, yielding a product with a different isomeric configuration. The neighboring proton is abstracted in the final step of the reaction. Thus, the E1 reaction does not require a strong base.

In the red chromophores of both Kaede and EosFP, the C=C double bond between His62-C_α and His62-C_β assumes a *trans*-configuration (*19*) [51,52]. By contrast, in the red chromophore of a variant of KikGR, the C=C double bond is in a *cis* configuration (*20*), indicating that the carbocation intermediate undergoes a structural rearrangement (Figure 4) [53]. Therefore, an E1-based reaction model has been proposed in order to comprehensively explain the structural data regarding photoconversion of the KikGR variant, as well as rationalize some inconsistencies in the proposed photoconversion mechanisms of Kaede and EosFP.

Conclusions

Our understanding of RFP structure and function has greatly advanced in the past several years, yet many controversies and riddles persist. On the basis of current knowledge, it may be possible to design new RFPs with improved photochemical properties. In addition, there have been a number of theoretical studies of the excited states of fluorescent proteins. In an effort to elucidate emission color-tuning mechanisms, for example, Hasegawa *et al.* performed a comparative study of the emission states of green-emitting (*Aequorea* GFP), orange-emitting (mKO), and red-emitting (DsRed) fluorescent proteins [54]. The authors used the QM/MM and SAC-CI methods to examine electrostatic and quantum mechanical interactions within the protein cavity, and found cancellation between the π skeleton extension (red shift) and the protein electrostatic potential (blue shift) to be the critical mechanism that determines the emission colors of RFPs. Another theoretical study that utilized electronic structure calculations has helped to clarify the nature of a blue intermediate in the process of DsRed chromophore formation [15•].

It is very likely that not only rational engineering but also random mutagenesis in conjunction with high-throughput screening techniques will be effective in the directed molecular evolution of RFPs [55•]. Furthermore, it is possible that newly cloned, naturally occurring RFPs will exhibit unprecedented photochemical properties. In this

context, we would like to recall the words expressed in 1999 by Dr. Roger Y. Tsien [56], regarding DsRed cloning [3•]: ''The ubiquity of these molecular tools makes it important to appreciate the interplay between sunlight and fluorescent proteins of anthozoan animals, and to consider the optimal use of these unique proteins in biological studies.''

Newly emerging RFPs will surely stimulate the imagination of many biologists, which will in turn spark an upsurge in demand for development of new variants and techniques. As a result, fluorescence microscopes will inevitably be equipped with special hardware and software functions to optimize their use. For example, a significant evolution in microscopy for deep-tissue and intravital imaging will be required for the efficient two-photon excitation of RFPs [57,58].

Acknowledgements

We thank Hiroko Sakurai and Hidekazu Tsutsui for help with preparing Figures 1 and 4, respectively, Mark A. Hink and Theodorus W.J. Gadella (both are from University of Amsterdam, Netherlands) for the data in Figure 2. This work was partly supported by grants from Japan Ministry of Education, Culture, Sports, Science and Technology Grant-in Aid for Scientific Research on Priority Areas (to A.M.) and GM073913 and CA164468 from the US National Institutes of Health (to V.V.V.).

References and recommended reading

Papers of particular interest, published within the period of review, have been highlighted as:

- • of special interest
- •• of outstanding interest

1. Tsien RY: **The green fluorescent protein**. *Annu Rev Biochem* 1998, **67**:509-544.

2. Mishin AS, Subach FV, Yampolsky IV, King W, Lukyanov KA, Verkhusha VV: **The first mutant of the Aequorea victoria green fluorescent protein that forms a red chromophore**. *Biochemistry* 2008, **47**:4666-4673.

3. • Matz MV, Fradkov AF, Labas YA, Savitsky AP, Zaraisky AG, Markelov ML, Lukyanov SA: **Fluorescent proteins from nonbioliminescent Anthozoa species**. *Nat Biotechnol* 1999, **17**:969-972.

A key paper demonstrating that anthozoan animals express spontaneously fluorescent proteins.

4. Day RN, Davidson MW: **The fluorescent protein palette: tools for cellular imaging**. *Chem Soc Rev* 2009, **38**:2887-2921.

5. Chudakov DM, Matz MV, Lukyanov S, Lukyanov KA: **Fluorescent proteins and their applications in imaging living cells and tissues**. *Physiol Rev* 2010, **90**:1103-1163.

6. Stepanenko OV, Stepanenko OV, Shcherbakova DM, Kuznetsova IM, Turoverov KK, Verkhusha VV: **Modern fluorescent proteins: from chromophore formation to novel intracellular applications**. *Biotechniques* 2011, **51**:313-314 316, 318 passim.

7. Subach FV, Verkhusha VV: **Chromophore transformations in red fluorescent proteins**. *Chem Rev* 2012, **112**:4308-4327.

8. •• Wachter RM, Watkins JL, Kim H: **Mechanistic diversity of red fluorescence acquisition by GFP-like proteins**. *Biochemistry* 2010, **49**:7417-7427.

References [7] and [8••] provide updated, detailed overviews of the chromophore transformations in GFP-like proteins.

9. Gross LA, Baird GS, Hoffman RC, Baldridge KK, Tsien RY: **The structure of the chromophore within DsRed, a red fluorescent protein from coral**. *Proc Natl Acad Sci USA* 2000, **97**:11990-11995.

10. Pletnev S, Subach FV, Dauter Z, Wlodawer A, Verkhusha VV: **Understanding blue-to-red conversion in monomeric fluorescent timers and hydrolytic degradation of their chromophores**. *J Am Chem Soc* 2010, **132**:2243-2253.

11. Strack RL, Strongin DE, Mets L, Glick BS, Keenan RJ: **Chromophore formation in DsRed occurs by a branched pathway**. *J Am Chem Soc* 2010, **132**:8496-8505.

12. Subach OM, Malashkevich VN, Zencheck WD, Morozova KS, Piatkevich KD, Almo SC, Verkhusha VV: **Structural characterization of acylimine-containing blue and red chromophores in mTagBFP and TagRFP fluorescent proteins**. *Chem Biol* 2010, **17**:333-341.

13. Subach OM, Cranfill PJ, Davidson MW, Verkhusha VV: **An enhanced monomeric blue fluorescent protein with the high chemical stability of the chromophore**. *PLoS ONE* 2011, **6**:e28674.

14. Subach FV, Malashkevich VN, Zencheck WD, Xiao H, Filonov GS, Almo SC, Verkhusha VV: **Photoactivation mechanism of PAmCherry based on crystal structures of the protein in the dark and fluorescent states**. *Proc Natl Acad Sci USA* 2009, **106**:21097-21102.

15. • Bravaya KB, Subach OM, Korovina N, Verkhusha VV, Krylov AI: **Insight into the common mechanism of the chromophore formation in the red fluorescent proteins: the elusive blue intermediate revealed**. *J Am Chem Soc* 2012, **134**:2807-2814.

References [10–14,15•] present evidence that the maturation of the DsRed-like red chromophore proceeds via a blue emitting intermediate that possesses a structure similar to the mTagBFP chromophore.

16. Shaner NC, Campbell RE, Steinbach PA, Giepmans BN, Palmer AE, Tsien RY: **Improved monomeric red, orange and yellow fluorescent proteins derived from Discosoma sp. red fluorescent protein**. *Nat Biotechnol* 2004, **22**:1567-1572.

17. Subach FV, Subach OM, Gundorov IS, Morozova KS, Piatkevich KD, Cuervo AM, Verkhusha VV: **Monomeric fluorescent timers that change color from blue to red report on cellular trafficking**. *Nat Chem Biol* 2009, **5**:118-126.

18. Remington SJ, Wachter RM, Yarbrough DK, Branchaud B, Anderson DC, Kallio K, Lukyanov KA: **zFP538, a yellow-fluorescent protein from Zoanthus, contains a novel three-ring chromophore**. *Biochemistry* 2005, **44**:202-212.

19. Kikuchi A, Fukumura E, Karasawa S, Mizuno H, Miyawaki A, Shiro Y: **Structural characterization of a thiazoline-containing chromophore in an orange fluorescent protein, monomeric Kusabira Orange**. *Biochemistry* 2008, **47**:11573-11580.

20. Shu X, Shaner NC, Yarbrough CA, Tsien RY, Remington SJ: **Novel chromophores and buried charges control color in mFruits**. *Biochemistry* 2006, **45**:9639-9647.

21. Yampolsky IV, Remington SJ, Martynov VI, Potapov VK, Lukyanov S, Lukyanov KA: **Synthesis and properties of the chromophore of the asFP595 chromoprotein from Anemonia sulcata**. *Biochemistry* 2005, **44**:5788-5793.

22. Chica RA, Moore MM, Allen BD, Mayo SL: **Generation of longer emission wavelength red fluorescent proteins using computationally designed libraries**. *Proc Natl Acad Sci USA* 2010, **107**:20257-20262.

23. Strack RL, Hein B, Bhattacharyya D, Hell SW, Keenan RJ, Glick BS: **A rapidly maturing far-red derivative of DsRed-Express2 for whole-cell labeling**. *Biochemistry* 2009, **48**:8279-8281.

24. Lin MZ, McKeown MR, Ng HL, Aguilera TA, Shaner NC, Campbell RE, Adams SR, Gross LA, Ma W, Alber T, Tsien RY: **Autofluorescent proteins with excitation in the optical window for intravital imaging in mammals**. *Chem Biol* 2009, **16**:1169-1179.

25. Morozova KS, Piatkevich KD, Gould TJ, Zhang J, Bewersdorf J, Verkhusha VV: **Far-red fluorescent protein excitable with red lasers for flow cytometry and superresolution STED nanoscopy**. *Biophys J* 2010, **99**:L13-L15.

26. • Chattoraj M, King BA, Bublitz GU, Boxer SG: **Ultra-fast excited state dynamics in green fluorescent protein: multiple states**

and proton transfer. *Proc Natl Acad Sci USA* 1996, **93**:8362-8367.
This report is the first to demonstrate the excited-state proton transfer in the neutral form of the *Aequorea* GFP.

27. Kogure T, Karasawa S, Araki T, Saito K, Kinjo M, Miyawaki A: **A fluorescent variant of a protein from the stony coral Montipora facilitates dual-color single-laser fluorescence cross-correlation spectroscopy**. *Nat Biotechnol* 2006, **24**:577-581.

28. Piatkevich KD, Hulit J, Subach OM, Wu B, Abdulla A, Segall JE, Verkhusha VV: **Monomeric red fluorescent proteins with a large Stokes shift**. *Proc Natl Acad Sci USA* 2010, **107**:5369-5374.

29. Shcherbakova DM, Hink MA, Joosen L, Gadella TW, Verkhusha VV: **An orange fluorescent protein with a large Stokes shift for single-excitation multicolor FCCS and FRET imaging**. *J Am Chem Soc* 2012, **134**:7913-7923.

30. Mizushima N, Yoshimori T, Levine B: **Methods in mammalian autophagy research**. *Cell* 2010, **140**:313-326.

31. • Katayama H, Yamamoto A, Mizushima N, Yoshimori T, Miyawaki A: **GFP-like proteins stably accumulate in lysosomes**. *Cell Struct Funct* 2008, **33**:1-12.
This paper highlights a biochemical difference between *Aequorea* GFPs and GFP-like proteins.

32. Katayama H, Kogure T, Mizushima N, Yoshimori T, Miyawaki A: **A sensitive and quantitative technique for detecting autophagic events based on lysosomal delivery**. *Chem Biol* 2011, **18**:1042-1052.

33. Lukyanov KA, Chudakov DM, Lukyanov S, Verkhusha VV: **Photoactivatable fluorescent proteins**. *Nat Rev Mol Cell Biol* 2005, **6**:885-891.

34. Lippincott-Schwartz J, Patterson GH: **Photoactivatable fluorescent proteins for diffraction-limited and super-resolution imaging**. *Trends Cell Biol* 2009, **19**:555-565.

35. Subach FV, Patterson GH, Manley S, Gillette JM, Lippincott-Schwartz J, Verkhusha VV: **Photoactivatable mCherry for high-resolution two-color fluorescence microscopy**. *Nat Methods* 2009, **6**:153-159.

36. • Subach FV, Patterson GH, Renz M, Lippincott-Schwartz J, Verkhusha VV: **Bright monomeric photoactivatable red fluorescent protein for two-color super-resolution sptPALM of live cells**. *J Am Chem Soc* 2010, **132**:6481-6491.
The authors achieved monitoring the dynamics of two different single transmembrane proteins fused to PATagRFP and PAGFP in the same cell.

37. Gunewardene MS, Subach FV, Gould TJ, Penoncello GP, Gudheti MV, Verkhusha VV, Hess ST: **Superresolution imaging of multiple fluorescent proteins with highly overlapping emission spectra in living cells**. *Biophys J* 2011, **101**:1522-1528.

38. Betzig E, Patterson GH, Sougrat R, Lindwasser OW, Olenych S, Bonifacino JS, Davidson MW, Lippincott-Schwartz J, Hess HF: **Imaging intracellular fluorescent proteins at nanometer resolution**. *Science* 2006, **313**:1642-1645.

39. Hess ST, Girirajan TP, Mason MD: **Ultra-high resolution imaging by fluorescence photoactivation localization microscopy**. *Biophys J* 2006, **91**:4258-4272.

40. Subach OM, Patterson GH, Ting LM, Wang Y, Condeelis JS, Verkhusha VV: **A photoswitchable orange-to-far-red fluorescent protein, PSmOrange**. *Nat Methods* 2011, **8**:771-777.

41. Subach OM, Entenberg D, Condeelis JS, Verkhusha VV: **A FRET-facilitated photoswitching using an orange fluorescent protein with the fast photoconversion kinetics**. *J Am Chem Soc* 2012, **134**:14789-14799.

42. Piatkevich KD, Verkhusha VV: **Advances in engineering of fluorescent proteins and photoactivatable proteins with red emission**. *Curr Opin Chem Biol* 2010, **14**:23-29.

43. Henderson JN, Ai HW, Campbell RE, Remington SJ: **Structural basis for reversible photobleaching of a green fluorescent protein homologue**. *Proc Natl Acad Sci USA* 2007, **104**:6672-6677.

44. Pletnev S, Subach FV, Dauter Z, Wlodawer A, Verkhusha VV: **A structural basis for reversible photoswitching of absorbance spectra in red fluorescent protein rsTagRFP**. *J Mol Biol* 2012, **417**:144-151.

45. Ando R, Hama H, Yamamoto-Hino M, Mizuno H, Miyawaki A: **An optical marker based on the UV-induced green-to-red photoconversion of a fluorescent protein**. *Proc Natl Acad Sci USA* 2002, **99**:12651-12656.

46. Wiedenmann J, Ivanchenko S, Oswald F, Schmitt F, Röcker C, Salih A, Spindler KD, Nienhaus GU: **EosFP, a fluorescent marker protein with UV-inducible green-to-red fluorescence conversion**. *Proc Natl Acad Sci USA* 2004, **101**:15905-15910.

47. Pakhomov AA, Martynova NY, Gurskaya NG, Balashova TA, Martynov VI: **Photoconversion of the chromophore of a fluorescent protein from Dendronephthya sp**. *Biochemistry (Mosc)* 2004, **69**:901-908.

48. Labas YA, Gurskaya NG, Yanushevich YG, Fradkov AF, Lukyanov KA, Lukyanov SA, Matz MV: **Diversity and evolution of the green fluorescent protein family**. *Proc Natl Acad Sci USA* 2002, **99**:4256-4261.

49. • Mizuno H, Mal TK, Tong KI, Ando R, Furuta T, Ikura M, Miyawaki A: **Photo-induced peptide cleavage in the green-to-red conversion of a fluorescent protein**. *Mol Cell* 2003, **12**:1051-1058.
This paper is the first to demonstrate β-elimination reaction for the green-to-red conversion.

50. Tsutsui H, Karasawa S, Shimizu H, Nukina N, Miyawaki A: **Semi-rational engineering of a coral fluorescent protein into an efficient highlighter**. *EMBO Rep* 2005, **6**:233-238.

51. Nienhaus K, Nienhaus GU, Wiedenmann J, Nar H: **Structural basis for photo-induced protein cleavage and green-to-red conversion of fluorescent protein EosFP**. *Proc Natl Acad Sci USA* 2005, **102**:9156-9159.

52. Hayashi I, Mizuno H, Tong KI, Furuta T, Tanaka F, Yoshimura M, Miyawaki A, Ikura M: **Crystallographic evidence for water-assisted photo-induced peptide cleavage in the stony coral fluorescent protein Kaede**. *J Mol Biol* 2007, **372**:918-926.

53. Tsutsui H, Shimizu H, Mizuno H, Nukina N, Furuta T, Miyawaki A: **The E1 mechanism in photo-induced beta-elimination reactions for green-to-red conversion of fluorescent proteins**. *Chem Biol* 2009, **16**:1140-1147.

54. Hasegawa JY, Ise T, Fujimoto KJ, Kikuchi A, Fukumura E, Miyawaki A, Shiro Y: **Excited states of fluorescent proteins, mKO and DsRed: chromophore-protein electrostatic interaction behind the color variations**. *J Phys Chem B* 2010, **114**:2971-2979.

55. • Subach FV, Piatkevich KD, Verkhusha VV: **Directed molecular evolution to design advanced red fluorescent proteins**. *Nat Methods* 2011, **8**:1019-1026.
The paper describes future perspectives of RFPs.

56. Tsien RY: **Rosy dawn for fluorescent proteins**. *Nat Biotechnol* 1999, **17**:956-957.

57. Kawano H, Kogure T, Abe Y, Mizuno H, Miyawaki A: **Two-photon dual-color imaging using fluorescent proteins**. *Nat Methods* 2008, **5**:373-374.

58. Drobizhev M, Makarov NS, Tillo SE, Hughes TE, Rebane A: **Two-photon absorption properties of fluorescent proteins**. *Nat Methods* 2011, **8**:393-399.

59. Nagai T, Yamada S, Tominaga T, Ichikawa M, Miyawaki A: **Expanded dynamic range of fluorescent indicators for Ca^{2+} by circularly permuted yellow fluorescent proteins**. *Proc Natl Acad Sci USA* 2004, **101**:10554-10559.